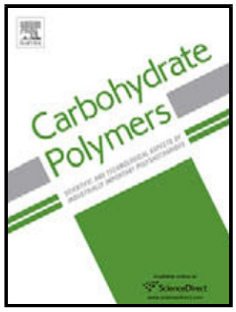

Title: Fabrication of bacterial cellulose/polyaniline/single-walled carbon nanotubes membrane for potential application as biosensor

Authors: Ashwak Jasim, Muhammad Wajid Ullah, Zhijun Shi, Xiao Lin, Guang Yang

PII: S0144-8617(17)30067-X
DOI: http://dx.doi.org/doi:10.1016/j.carbpol.2017.01.056
Reference: CARP 11934

To appear in:

Received date: 25-11-2016
Revised date: 25-12-2016
Accepted date: 15-1-2017

Please cite this article as: Jasim, Ashwak., Ullah, Muhammad Wajid., Shi, Zhijun., Lin, Xiao., & Yang, Guang., Fabrication of bacterial cellulose/polyaniline/single-walled carbon nanotubes membrane for potential application as biosensor.*Carbohydrate Polymers* http://dx.doi.org/10.1016/j.carbpol.2017.01.056

Fabrication of bacterial cellulose/polyaniline/single-walled carbon nanotubes membrane for potential application as biosensor

Ashwak Jasim[¥], Muhammad Wajid Ullah[¥], Zhijun Shi, Xiao Lin, Guang Yang*

Department of Biomedical Engineering, College of Life Science and Technology, Huazhong University of Science and Technology, Wuhan 430074, PR China

*Corresponding author

Guang Yang

Email: yang_sunny@yahoo.com

[¥]These authors contributed equally to this work.

Graphical Abstract

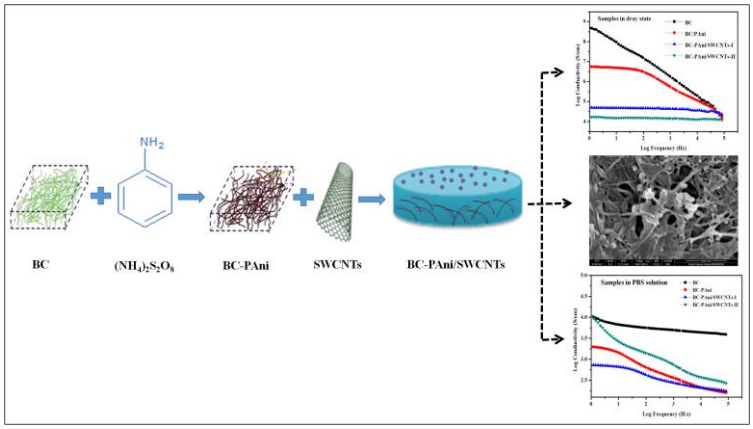

Highlights

- Development of electrically conductive BC-PAni/SWCNTs composite membrane
- Dense array of PAni on BC fibers and uniform distribution of SWCNTs
- Enhanced conductivity by increased concentrations of SWCNTs
- Improved thermal properties of BC-PAni/SWCNTs composite
- Potential applications of BC-PAni/SWCNTs in biosensors

Abstract

Electrically conductive polymeric membranes of BC with polyaniline (PAni) were fabricated through *ex situ* oxidative polymerization. PAni was densely arrayed along BC fibers and SWCNTs were uniformly distributed in the composites as confirmed by field emission scanning electron microscopy (FE-SEM). Fourier transform-infrared (FT-IR) spectra of the composite membranes exhibited characteristic peaks for specific functional groups of PAni and SWCNTs besides BC. X-ray diffraction (XRD) analysis indicated the presence of specific peaks for BC, PAni, and SWCNTs in the composites. The conjugated backbone of PAni and SWCNTs contributed to improve the degradation temperatures from 232°C for BC to 260°C, 302°C, and 310°C for

BC-PAni, BC-PAni/SWCNTs-I (0.05 mg/mL), and BC-PAni/SWCNTs-II (0.1 mg/mL) composites, respectively. The electrical conductivity of BC was enhanced to 1.04×10^{-3} S/cm, 4.64×10^{-3} S/cm, and 1.41×10^{-2} S/cm upon doping with PAni, and 0.05 mg/mL and 0.1 mg/mL SWCNTs, respectively in dry state which was further increased to 4.02×10^{-2} S/cm, 3.03×10^{-2} S/cm, 5.93×10^{-1} S/cm, and 7.36×10^{-1} S/cm, respectively in PBS solution. These membranes can potentially be used for applications requiring biocompatibility and electrical conductivity such as biological and chemical sensors.

Keywords: Bacterial cellulose, Polyaniline, Single-walled carbon nanotubes, Conducting composites, Biosensors

1. Introduction

Bacterial cellulose (BC) is produced by several genera (e.g. *Acetobacter*, *Rhizobium*, *Agrobacterium*, *Aerobacter*, *Achromobacter*, *Azotobacter*, *Salmonella*, *Escherichia*, and *Sarcina*) as well as cell-free system and represent the purest form of cellulose compared to plant cellulose (Ullah, Ul-Islam, Khan, Kim, & Park, 2016a; Ullah, Khattak, Ul-Islam, Khan, & Park, 2016b; Seo et al., 2014). It possesses a three-dimensional network of nanofibers formed by self-assembly and shows unique structural and physico-mechanical features that make it an attractive material for various applications (Ul-Islam, Khattak, Ullah, Khan, & Park, 2014; Czaja, Krystynowicz, Bielecki, & Brown, 2006). It serves as support materials for broad spectrum applications owing to its unique features. Applications of BC in medical fields, for example artificial skin, artificial blood vessels, scaffolds for tissue engineering, and wound dressing; food items, cosmetics, separation membrane, drug

delivery, enzyme immobilization, and optoelectronics have already been reported (Ullah, Ul-Islam, Khan, Kim, & Park, 2016b, 2015; Khan, Ul-Islam, Khattak, Ullah, & Park, 2015; Feng, Zhang, Shen, Yoshino, & Feng 2012; Czaja et al., 2006). However, the broad spectrum applications of BC have been limited by several inadequacies associated with BC such as low biocompatibility and lack of bactericidal, antioxidant, conducting and electromagnetic properties etc. (Kim et al., 2011). These limitations necessitate the development of composites of BC with other materials to impart such properties to BC.

BC can exist in the form of hydrogels containing large amounts of water, membranes, fibers, small pellicle, large sheets, slurry, and powder etc. (Shi et al., 2016). The BC fibrils are about 100 times thinner that those of plant cellulose and are interconnected through inter– and intra–molecular hydrogen bonding (Ul-Islam et al., 2013; Klemm, Schumann, Udhardt, & Marsch, 2001). These fibrils are loosely arranged and contain empty spaces in the form of pores that result in extended surface area and highly porous matrix (Dahman, 2009; Meftahi et al., 2010). These pores can accommodate both liquids (e.g. media components) and solids (e.g. polymers molecules, nanoparticles etc.) and thus it can support the synthesis of nano– and polymeric-composites with biocompatible, bactericidal, and electro-conductive materials for various biomedical and optoelectronics applications (Ul-Islam, Khan, Ullah, & Park, 2016). To date, several strategies (e.g. *in situ*, *ex situ*, and regeneration method etc. have been developed which utilized plant cellulose, regenerated cellulose, and cellulose derivatives in combination with several polymers and conductive materials for the synthesis of electro-conductive composite materials (Ifuku, Tsuji, & Morimoto, 2007; Nogi & Yano, 2008).

Composites of BC have been developed by blending its nanofibrils with several polymeric matrices (Trovatti, Oliveira, & Freire, 2010) or by *in situ* polymerization of monomers on the BC nanofibers (Hobzova, Duskova-Smrckova, Michalek, Karpushkin, & Gatenholm, 2012) to enhance its biocompatibility. Similarly, in order to enhance the electrical conductivity of BC, its nanofibrils have been coated with intrinsically conductive polymers. For instance, polyaniline (PAni) is a well known and extensively explored conductive polymers due to its pH sensitivity and ease of synthesis which makes it an attractive material for application in chemical sensors and antistatic coatings (Maziarz, Lorenz, White, & Wood, 2000). PAni and its derivatives are attractive candidates owing to their stability and processability at relatively low production cost. BC-PAni composites have received immense consideration as conductive and flexible electrode materials in electrical devices applications (Qaiser, Hyland, & Patterson, 2011). Several strategies have been developed for the synthesis of such composites: for example, simple *in situ* polymerization (Wang et al., 2012; Shi, Zang, & Jiang, 2012), and *in situ* oxidative polymerization of aniline with ammonium persulfate (APS) as an oxidant and BC as template (Hu, Chen, Yang, Liu, & Wang, 2011). Lee and Hong investigated the influence of reaction time and different types of protonic acids on the electrical conductivity of wet BC-based composite with PAni (Lee & Hong, 2000). Although, composites of BC with PAni prepared through different strategies have shown considerable electrical conductivity, it can be further enhanced by using other materials possessing intrinsic electrical conductivity. For example, carbon nanotubes (CNTs) can be doped into the matrix as these posses high surface area, tunable surface function, high electrical conductivity, and environmental stability. Further, recent studies have reported that incorporation of CNTs into the matrix enhance the

mechanical properties of the polymer (Cucchi et al., 2009). Similarly, several studies have reported the incorporation of CNTs into BC using the surfactant cetyl trimethyl ammonium bromide (CTAB) through *ex situ* dipping (Yoon, Jin, Kook, & Pyun, 2006) or PAni by adding dispersed SWCNTs to the polymer solution or by chemical polymerization of aniline in the presence of SWCNTs (Huang, Virji, Weiller, Kaner, 2003).

In the current study, we prepared a BC-PAni/SWCNTs composite in a two step process to enhance the biocompatibility and electrical conductivity of BC. In first step, BC-PAni composite was prepared by *in situ* polymerization of aniline on BC fibers. It was followed by doping of SWCNTs in to the BC-PAni matrix. The morphological changes occurring during the polymerization process were monitored by FE-SEM, FTIR, and XRD analyses. Electrical conductivity measurement was carried out to investigate the electrical properties and electrochemical performance of BC-PAni/SWCNTs nanocomposite membranes. The thermal properties of the composite membranes were investigated through TGA. This combination of BC with electroactive and biocompatible polymer (PAni) and inherently conductive material (SWCNTs) may serve as excellent electrochemical and biocompatible membrane material for potential applications in biosensors development.

2. Experimental

2.1. Materials

The chemical reagents including glucose, yeast extract, peptone, disodiumphosphate, and citric acid were purchased from Sigma-Aldrich (St. Louis, MO, USA). Aniline, ammonium peroxydisulfate $(NH4)_2S_2O_8$) of analytical grade were purchased from Sinopharm Chemical Regents Co., Ltd. (Shanghai, China).

Single walled carbon nanotubes (outer diameter: <2 nm; length: 5–15 μm) were purchased from Chengdu Organic Chemicals Co. Ltd. (Chengdu, China). All the reagents were utilized in the experiments without any additional processing.

2.2. Microorganism and cell culture

Gluconacetobacter xylinum (ATCC53582) was used for the biosynthesis of BC pellicles as reported previously (Shi et al., 2012). Briefly, the bacterium was cultured in a Hestrin and Schramm (HS) medium containing glucose 20 gL^{-1}, yeast extract 5 gL^{-1}, peptone 5 gL^{-1}, disodiumphosphate 2.7 gL^{-1}, and citric acid 1.15 gL^{-1}. The pH of the medium was adjusted to 5.0 with 1.0 M NaOH. The medium was sterilized for 15 min at 15 psi and 121°C. A few colonies from *G. xylinum* culture plate were inoculated into 100 mL of broth medium in a 250 mL Erlenmeyer flask and incubated for 24 h at 30°C under shaking conditions. Thereafter, a small volume (3-5% v/v) from this freshly prepared pre-culture was inoculated into a new HS medium and incubated statically at 30°C for 6-10 days. As a result BC membrane was produced at the surface of the culture medium. The BC produced was harvested and treated with 0.3 M NaOH for 15 min at 15 psi at 121°C to disrupt and dissolve the cell debris as reported previously (Ul-Islam et al., 2013). The treated BC was then washed thoroughly with deionized distilled water until the pH became neutral, and was stored in distilled water at 4°C for synthesis of composite and analysis.

2.3. Development of BC-PAni composite

A BC slurry was prepared by homogenizing BC in 20 wt% ammonium peroxydisulfate solution (APS) for 24 h at room temperature. The slurry was then immersed in an aniline/ethanol mixture (1:10) at ambient temperature and stirred for 24 h. A schematic diagram of the process of aniline polymerization is shown in Fig. 1. During stirring, the aniline was adsorbed on to the surface of BC fibers that resulted in

formation of black-colored BC-Pani slurry. The slurry was centrifuged at 8,000 rpm for 20 min. Thereafter, dialysis was performed to wash BC-Pani composite and remove the unbound aniline. For this purpose, the composite was packed in dialysis bag (8,000-14,000 Da) and placed in distilled water for 48 h at room temperature while changing the water after every 6-12 h. Finally, the BC-Pani composite was harvested and preserved at 4°C for further use.

2.4. Development of BC-PAni/SWCNTs composite

The as-received pristine SWCNTs (97%) were dispersed in deionized distilled water with a cationic CTAB surfactant (0.3 wt% in H_2O) through sonication (Kodo Technical Research Co., Japan) using nominal frequency of 28 kHz and a power of 600W for 1 h at 25°C. Thereafter, different concentrations of SWCNTs (i.e. 0.05 mg/mL and 0.10 mg/mL) were mixed with 3 g of BC-PAni slurry prepared in 50 mL of distilled water at room temperature. The composite samples obtained by mixing 0.05 mg/mL and 0.10 mg/mL of SWCNTs were designated as BC–PAni/SWCNTs-I and BC–PAni/SWCNTs-II, respectively. The mixture was stirred at 100 rpm for 30 min at room temperature. Thereafter, the mixture was transferred to a vacuum filtration assembly and filtered for 1 h at room temperature. The synthesized BC-PAni/SWCNTs membrane was then freeze-dried and stored at room temperature for analysis and characterization.

2.5. Characterization of pure BC and BC-PAni, BC-PAni/SWCNTs-I, and BC-PAni/SWCNTs-II composites

The synthesized BC and BC-PAni, BC-PAni/SWCNTs-I, and BC-PAni/SWCNTs-II composites were characterized through different techniques for various features. The surface morphology of freeze-dried samples was observed through FE-SEM. Briefly, samples were fixed on a brass holder and coated with gold

on a Cu SEM disk and analyzed through a Nova NanoSEM450 FE-SEM (Nova NanoSEM450, FEI, Holand). FTIR spectra of freeze-dried samples was recorded using a Vertex FTIR spectrophotometer (FTIR, VERTEX 70, Germany; spectral range 4000-500cm^{-1}; beam splitter: Ge-coated on KBr; detector: DTGS; resolution: 0. 25 cm^{-1} (step selectable)] to determine the chemical structure of the composite films and possible interactions between their components. The obtained IR data was transferred to PC to acquire spectra. The XRD pattern of all samples were recorded using an X-ray diffractometer with an X-ray generator (3 kW) and anode (LFF Cu). The radiation was CuK-α at 1.54 A°, the X-ray generator tension and current was 40 kV and 30 mA, respectively, and the angle of scanning varied from 0 to 80°. The electrical conductivities of all samples were measured using Potentiostats-Electrochemistry Workstation (Par 2273, USA). The samples were placed between Pt electrodes by measuring the current in a voltage range at 1 Hz–100 kHz. Liner sweep voltammetry was performed in a standard three-electrode cell setup while utilizing the composite films, platinum plate and Ag/AgCl as working electrode, counter electrode, and reference electrode, respectively. The voltammetrograms were obtained in dry state and in PBs solution at potentials ranging from –0.8 to 0.0 V for BC-PAni/SWCNTs with different scan rates. The thermogravimetric analysis of all samples was carried out using a thermogravimetric/differential analyzer (Q50 thermo balance). The thermogram for TGA was obtained in the range of 30-600°C under a nitrogen atmosphere with a temperature increase of 20°C/min.

3. Results and Discussion

3.1. Development of BC-PAni/SWCNTs nanocomposite

Bacterial cellulose pellicles produced by *G. xylinum* were used to synthesize flexible BC-PAni/SWCNTs composite membranes. The synthesis was carried out in two phases: *ex situ* oxidative polymerization of PAni on the surface of BC fibers followed by the addition of various concentrations of SWCNTs (Fig. 1). The aniline hydrochloride permeated through the inner network of BC and coated. At the same time, the hydroxyl groups (–OH) present on the surface of BC interact with the amine groups of aniline to form the hydrogen bonds which ensure the uniform distribution of aniline on the surface of BC nanofibers (Marins et al., 2011). Once immersed in the ammonium persulfate (oxidant) solution in an acidic medium, the monomers polymerize in the network of BC as shown in Fig. 1A (Baslak et al., 2015). Prior to addition into the BC-PAni composite, suspensions of SWCNTs (0.05 mg/mL and 0.1 mg/mL) were prepared in CTAB surfactant through sonication for 1 h at room temperature to ensure the uniform distribution of nanoparticles in the composite. The synthesized BC-PAni/SWCNTs composite membranes were removed from the mixture and rinsed several times with deionzied distilled water to remove the surfactant and unbound nanoparticles from the its surface. Finally, the membrane was vacuum-dried and stored for further analysis.

3.2. Morphological analysis of pure BC and BC-PAni, BC-PAni/SWCNTs-I, and BC-PAni/SWCNTs-II composites

Pure bacterial cellulose appeared whitish in color and very light-weighted upon freeze-drying while the BC-PAni, and BC-PAni/SWCNTs-I and BC-PAni/SWCNTs-II composite membranes were bluish-black in color. Morphological analyses of freeze-dried BC and BC-PAni, BC-PAni/SWCNTs-I, and BC-PAni/SWCNTs-II composite membranes were carried out via FE-SEM to investigate the structure of pure BC and synthesis of its composites with PAni and SWCNTs.

Freeze-drying, involving the direct conversion of ice to vapors, maintains the pore-geometry of the sample (Ul-Islam, Shah, Ha, & Park, 2011).

Fig. 2 shows the SEM micrographs of pure BC and BC-PAni, BC-PAni/SWCNTs-I, and BC-PAni/SWCNTs-II composites. SEM micrograph of pure BC showed a three dimensional arrangement of long chain web-shaped cellulose fibrils with high aspect ratio (Fig. 2A) (Ullah et al., 2016a; Khattak et al., 2015). The fibrils were randomly distributed in BC forming pores of different sizes in the matrix. Fig. 2B shows the morphology of purified SWCNTs powder. Fig. 2C shows the polymerization of PAni which is entangled with BC fibrils. The fibrils arrangement in BC-PAni is quite different from that of pure BC and is more compact, thus it will affect its several features, for example, thermal and mechanical properties etc. The impregnation of SWCNTs into the BC matrix is shown in Fig. 2D and 2E. The morphology of SWCNTs doped BC is quite different from pure BC and the one doped with PAni. The concentration of nanotubes in the composite increased when the content of SWCNTs was increased from 0.05 mg/mL to 0.1 mg/mL as shown in Fig. 2D and 2E, respectively. The hydroxyl groups from BC in the BC-PAni membrane combine with the SWCNTs. The SWCNTs are uniformly distributed throughout the surface and show very little or no agglomeration. When compared to BC-PAni/SWCNTs-I, the number of SWCNTs nanoparticles were higher in BC-PAni/SWCNTs-II. Overall, the SEM micrographs showed a reticulated cellulose fibril arrangement with clear variations in size and density for both concentrations of SWCNTs. The entanglement of PAni along the BC fibrils and non-agglomeration of SWCNTs in BC-PAni matrix is a good indicator for the enhanced biological and conductive properties of the composite, respectively.

3.3. FTIR characterization of pure BC and BC-PAni, BC-PAni/SWCNTs-I, and BC-PAni/SWCNTs-II composites

FTIR is a useful spectroscopic technique to investigate the existence of target functional groups and the nature of chemical bonds linking them together in a molecule, polymer, or a composite (Ul-Islam et al., 2013; Ullah et al., 2016b). In the current study pure BC, BC-PAni, BC-PAni/SWCNTs-I, and BC-PAni/SWCNTs-II composites were analyzed through FTIR to verify the successful impregnation of PAni and SWCNTs into the BC matrix.

Fig. 3 shows the FTIR spectra of pure BC, BC-PAni, BC-PAni/SWCNTs-I, and BC-PAni/SWCNTs-II composites. The FT-IR spectrum of pure BC contained all the characteristic peaks for all chemical groups in cellulose and thereby confirmed the basic stricture of pure cellulose. Mainly, two broad characteristic peaks for –OH stretching appeared at 3332 cm-1 and 2896 cm-1, respectively in FT-IR spectra of pure cellulose which is in agreement with previous study (Ul-Islam et al., 2013). The presence of the –CH group was further confirmed by the appearance of several peaks corresponding to –CH bending vibrations at 1450–1200 cm−1 (Ul-Islam et al., 2011). Further, an intense peak appeared at 1,651 cm−1 that confirmed the presence of glucose carbonyl group in cellulose (Ul-Islam et al., 2011). Two more characteristic peaks appeared at 1,427 cm−1 and 1,371 cm−1 which demonstrate the symmetric deformation and bending vibration of CH group, respectively (Ullah et al., 2016a). The peak for C–O–C stretching appears at 1,035 cm−1 as reported previously (Shah, Ha, & Park, 2010). The FT-IR spectra of BC-PAni showed two strong additional peaks at 1555cm^{-1} and 1502 cm^{-1} which were assigned to quinone and benzene rings stretching oscillation, respectively as reported previously (Shi et al., 2012; Kang, Neoh, & Tan, 1998). The conductive PAni usually consists of about equal amounts of

quinonoid and benzenoid units and posses approximately equal intensities for both the 1555 cm^{-1} and 1502 cm^{-1} absorption bands (Kang et al., 1998). The stronger intensity of peak at 1502 cm^{-1} compared to peak at 1555 cm^{-1} demonstrate the presence of higher amount of benzenoid units compared to quinonoid units. Usually, the BC-PAni which have equal quinonoid and benzenoid units as indicated by their similar band intensities indicate that they possess a similar structure to that of a conductive PAni and thus the corresponding BC-PAni composite is expected to have better electrical conductivity. Usually the intensity of peak at 3400 cm^{-1} due to OH group in BC is reduced or sometimes disappeared completely when PAni is incorporated into the BC matrix. Further, the absorption spectra of BC-PAni composite did not show any N-H stretching absorption as reported previously (Shi et al., 2012). Thus, BC may have reacted via dehydration-condensation with PAni and may result in the disappearance of O-H and N-H bonds. The FT-IR spectra of BC-PAni/SWCNTs-I, and BC-PAni/SWCNTs-II composites showed additional peaks around cm^{-1} which can be attributed to benezne group (Yoon et al., 2006). However, the peak for C–C functional group is not obvious probably due to low concentration of SWCNTs. These results show the successful impregnation of PAni and SWCNTs into the BC matrix. However, further investigation is required to confirm the presence of SWCNTs in the matrix. It can be assumed that the –OH groups present on the surface of BC contributed to the uniform distribution of PAni which interact with aniline monomer and thus serve as a substrate for BC-PAni composite synthesis.

3.4. X-ray diffraction (XRD)

BC is a semi-crystalline material that demonstrate three characteristic crystallinic peaks when examined through XRD. Crystallinity and strength of hydrogen bonding accounts for morphological changes in the microstructure of BC

(Shezad, Khan, Khan, & Park, 2010). These structural changes in the microstructure of BC can be monitored by the X-ray diffraction analysis. Therefore, XRD analyses of was carried out for BC, BC-PAni, BC-PAni/SWCNTs-I, and BC-PAni/SWCNTs-II composites to investigate the micro structural changes in the BC caused by the adsorption and penetration of PAni and different concentrations of SWCNTs.

A comparative study of the XRD spectra of the extended linear scanning (10–70°) of BC, BC-PAni, BC-PAni/SWCNTs-I, and BC-PAni/SWCNTs-II composites is shown in Fig. 4. The XRD spectrum of BC showed two broad peaks at 2θ 14.2° and 22.7° along with a weak middle peak at 16.6° corresponding to the (1-10), (200), and (110) crystallinic planes of the cellulose 1β structure which is in agreement with previous studies (Ullah et al., 2015; French, 2014). In contrast, the BC-PAni composite showed two additional peaks at 2θ 12° and 22°. These peaks are broad and cause a decrease in the extent of order of cellulose probably due to a weak acidic degradation rather than a direct effect of PAni. Similarly, the BC-PAni/SWCNTs showed an additional sharp peak with high intensity at 2θ 25° and a lower intensity peak at 2θ 43° which are consistent with previous studies. Compared with BC and BC-PAni, the peak intensity at 2θ 26° gradually enhanced with increasing SWCNTs concentration which can be attributed to the overlapping of BC-PAni with SWCNTs.

3.5. Electrical conductivity of BC and BC-PAni, BC-PAni/SWCNTs-I, and BC-PAni/SWCNTs-II composites

Electrical conductivity measurements were carried out for pure BC, BC-PAni, BC-PAni/SWCNTs-I, and BC-PAni/SWCNTs-II nanocomposite films in dry state and in PBS solution using the three-probe method. The conductivity test was performed at room temperature in a potentiostatic electrochemical workstation (Par

2273, USA) with different concentrations of SWCNTs as the working electrode, a platinum electrode as the counter electrode, and Ag/AgCl electrode as the reference electrode, whereas the pure BC film was used as insulator.

A considerable increase in the electrical conductivity of any material from insulating to the semiconductor is considered significant. Electrical conductivity of PAni largely depends on the degree of polymerization, oxidation state, particle morphology, crystallinity, interior intra-chain interactions, molecular weight (Yang, Chen, Ren, Zhang, & Yang, 2015). Fig. 5A shows the electrical conductivities of all samples in dry state. Specifically, electrical conductivity of a BC sheet (2×1 cm^2) was shown to be 2.7×10^{-4} S/cm and thus behaved as nearly insulator (Khan et al., 2015). The addition of polyaniline to the BC matrix significantly increased its electrical conductivity and reached to 1.04×10^{-3} S/cm. Similarly, the direct current electrical conductivity (σ DC) of BC-PAni/SWCNTs was recorded to be 4.64×10^{-3} S/cm.

In case of ionic conductivity with PBS solution, the BC, BC-PAni, and BC-PAni, and BC-PAni/SWCNTs working electrode were connected to the electrode site through a connector. The counter electrode was connected to a platinum foil and placed in a glass container. A Ag/AgCl reference electrode and a neutral microelectrode tip were immersed in the glass container for pure BC in PBS solution. Fig. 5B shows the electrical conductivities of all samples in dry state. The electrical conductivity of the pure BC in PBS solution was recorded to be 4.02×10^{-2} S/cm which increased to 3.03×10^{-2} S/cm after polymerization with PAni. The electrical conductivity was further increased to 5.08×10^{-1} S/cm after impregnation with SWCNTs as shown in Fig. 5B. The dispersed SWCNTs improved the electrical conductivity of the BC-PAni matrix probably due to the formation of conductive networks throughout the insulating BC matrix. The conductive

property of the BC-based nanocomposite membrane makes it a promising candidate for potential applications in biosensors and tissue engineering (e.g. development of electroactive hydrogels).

3.6. Linear sweep voltammetry

The linear sweep voltammetry is a voltammetric method that involves the measuring of current at a working electrode while the potential between the working and reference electrode is swept linearly with respect to time. During this process, the oxidation or reduction of species under observation is registered as a peak at the potential at which the species begin to be oxidized or reduced in an aqueous solution. This process is performed in a standard three-electrode cell setup utilizing with the nanocomposite films as the working electrode.

In the current study, BC, BC-PAni, BC-PAni/SWCNTs-I, and BC-PAni/SWCNTs-II nanocomposite films were used separately as working electrode while a platinum plate and Ag/AgCl were used as counter and reference electrodes, respectively. The measurements were carried out in PBS solution at potentials ranging from −0.1 to 0.1V for BC-PAni, BC-PAni/SWCNTs-I, and BC-PAni/SWCNTs-II nanocomposite films in 5% of PBS solution as shown in Fig. 6. The results showed that BC-PAni/SWCNTs-I, and BC-PAni/SWCNTs-II nanocomposite films were more electroactive than the BC-PAni composite, particularly showing the coupled oxidation and reduction peaks between −0.1 to 0.1V (vs. Ag/AgCl). This enhanced electroactivity can be attributed to the acid treatment creating more functional groups on the SWCNTs which support the FTIR analysis as shown in Fig. 3. (Shi et al., 2012).

3.7. Thermal stability of pure BC, and BC-PAni, BC-PAni/SWCNTs-I, and BC-PAni/SWCNTs-II composite films

The commercial applications of BC are highly dependent on its thermal stability, especially at elevated temperatures. Therefore, the thermal behavior of BC, BC-PAni, BC-PAni/SWCNTs-I, and BC-PAni/SWCNTs-II nanocomposite films was investigated using TGA. The TGA thermograms of BC and BC-PAni, BC-PAni/SWCNTs-I, and BC-PAni/SWCNTs-II composite films are shown in Fig. 7. The thermal degradation of BC involves three processes: dehydration, depolymerization, and decomposition of glycosyl units followed by the formation of a charred residue (George, Ramana, Bawa, & Siddaramaiah, 2011).

Two major weight loss zones can be observed in all these curves (Ullah et al., 2016a). About 10-12% weight loss occurred at a temperature range of 90-100°C for pure BC. In contrast, only 8%, 6.5%, and 6% weight loss occurred for BC-PAni, BC-PAni/SWCNTs-I, and BC-PAni/SWCNTs-II nanocomposite films at this temperature. The weight loss at this temperature can be attributed to the loss of moisture content adsorbed on the surface and the inter layer-coordinate water molecules (Darder, Colilla, & Ruiz-Hitzky, 2003; Khan & Park, 2008). The relatively higher weight loss for the pure BC at this temperature range may be due to its higher water holding capacity as compared to the BC-PAni, BC-PAni/SWCNTs-I, and BC-PAni/SWCNTs-II nanocomposites. The second phase of degradation started above 225°C in all samples. In this phase, the degradation of main cellulose skeleton takes place (Li, Kim, Lee, Kee, & Oh, 2011). A maximum weight loss was recorded for all samples during this phase. The weight loss for pure BC was about 65% during this phase as shown in Fig. 7 which indicates the degradation of main cellulose skeleton (Li et al., 2010). In contrast, the weight loss during this phase for BC-PAni, BC-PAni/SWCNTs-I, and BC-PAni/SWCNTs-II nanocomposites was comparatively lower than for pure BC. Moreover, the weight loss decreased for BC-PAni and with increasing concentrations

of SWCNTs in the nanocomposites and and was found to be about 32%, 25%, and 22% for BC-PAni, BC-PAni/SWCNTs-I, and BC-PAni/SWCNTs-II nanocomposites, respectively. Furthermore, the degradation temperatures for the BC-PAni, BC-PAni/SWCNTs-I, and BC-PAni/SWCNTs-II nanocomposites during this phase were different from that of pure BC as shown in Fig. 7. The degradation of pure BC started at 232°C, which was extended to 260°C for BC-PAni and further increased to 302°C and 310°C for BC-PAni/SWCNTs-I, and BC-PAni/SWCNTs-II nanocomposites, respectively. These results indicate that PAni and SWCNTs are thermally stable as the onset of their degradation occurs at a temperature of more than 600°C. The incorporation of PAni and SWCNTs into the BC matrix during composite synthesis is expected to improve the overall thermal stability of BC because their presence inside and on the surface of the BC can protect the cellulose chains against thermal shock. This protection ultimately results in shifting the degradation towards higher temperatures and reduction in their weight loss. Moreover, the hydrogen bonding between BC and PAni and SWCNTs groups may also lead to an improvement in the thermal properties of the BC chains.

4. Conclusions

In this work, a systematic study for the production of BC-PAni/SWCNTs nanocomposite membrane was performed through *in situ* oxidative polymerization of aniline. The structural, morphological and conductivity studies were performed for pure BC, BC-PAni, and BC-PAni/SWCNT composites. The results showed that nanocomposites membrane was successfully synthesized by oxidation polymerization method. FE-SEM showed the coating of PAni layer along the BC fibers and uniform distribution of SWCNTs. FTIR and XRD analyses confirmed the chemical and polymorphic structures of pure BC and its composites with PAni and SWCNTs. TGA

analysis demonstrated that thermal stability of BC was significantly improved upon the addition of PAni and SWCNTs into its matrix. The BC-PAni/SWCNTs composite showed an improved electrical conductivity and thus can be used in several potential applications in the biomedical field such as biosensors, biofuel cells, and bio-electronic devices etc.

Acknowledgements

This work was supported by National Natural Science Foundation of China (21574050, 31270150, 51603079), China Postdoctoral Science Foundation (2016M602291, 2015M572132), Fundamental Research Funds for the Central Universities, Open Research Fund of State Key Laboratory of Polymer Physics and Chemistry, Changchun Institute of Applied Chemistry, Chinese Academy of Sciences.

References

Baslak, C., Demirel, M., Karaman, M., Kus, M., Cengeloglu, Y., & Ersoz, M. (2015). Biocompatible multi-walled carbon nanotube–CNT quantum dot–polymer hybrids for medical applications. *Journal of Luminescence*, 160, 9-15.

Cucchi, I., Boschi, A., Arosio, C., Bertini, F., Freddi, G., & Catellani, M. (2009). Bio-based conductive composites: preparation and properties of polypyrrole (PPy)-coated silk fabrics. *Synthetic Metals*, 159, 246–253.

Czaja, W., Krystynowicz, A., Bielecki, S., & Brown, R. M. (2006). Microbial cellulose – the natural power to heal wounds. *Biomaterials*, 27, 145–151.

Dahman, Y. (2009). Nanostructured biomaterials and biocomposites from bacterial cellulose nanofibers. *Journal of Nanoscience and Nanotechnology*, 9, 5105–5122.

Darder, M., Colilla, M., & Ruiz-Hitzky, E. (2003). Biopolymer-clay nanocomposites based on chitosan intercalated in montmorillonite. *Chemistry of Materials*, 15, 3774–3780.

Feng, Y., Zhang, X., Shen, Y., Yoshino, K., & Feng, W. (2012). Amechanically strong ,flexible and conductive film based on bacterial cellulose/grapheme nanocomposite. *Carbohydrate Polymers*, 87, 644–649.

French, A. D. (2014). Idealized powder diffraction patterns for cellulose polymorphs. *Cellulose*, 21, 885–896.

George, J., Ramana, K. V., Bawa, A. S., & Siddaramaiah. (2011). Bacterial cellulose nanocrystals exhibiting high thermal stability and their polymer nanocomposites. *International Journal of Biological Macromolecules*, 48, 50–57.

Hobzova, R., Duskova-Smrckova, M., Michalek, J., Karpushkin, E., & Gatenholm, P. (2012). Methacrylate hydrogels reinforced with bacterial cellulose. *Polymer International*, 61, 1193–1201.

Hu, W., Chen, S., Yang, Z., Liu, L., & Wang, H. (2011). Flexible electrically conductive nanocomposite membrane based on bacterial cellulose and polyaniline. *Journal of Physical Chemistry B*, 115, 8453–8457.

Huang, J. X., Virji, S., Weiller, B. H., & Kaner, R. B. (2003). Polyaniline nanofibers: facile synthesis and chemical sensors. *Journal of American Chemical Society*, 125, 314–315.

Ifuku, S., Tsuji, M., & Morimoto, M. (2009). Synthesis Of Silver Nanoparticles Templated By TEMPO-Mediated Oxidized Bacterial Cellulose Nanofibers. *Biomacromolecules*, 10, 2714-2717.

Kang, E. T., Neoh, K. G., & Tan, K. L. (1998). Polyaniline: A polymer with many interesting intrinsic redox states. *Progress in Polymer Science*, 23, 277-324.

Khan, S., Ul-Islam, M., Khattak, W. A., Ullah, M. W., & Park, J. K. (2015). Bacterial cellulose–poly(3,4-ethylenedioxythiophene)–poly (styrenesulfonate) composites for optoelectronic applications. *Carbohydrate Polymers*, 127, 86–93.

Khan, T., & Park, J. K. (2008). The structure and physical properties of glucuronic acid oligomers produced by a *Gluconacetobacter hansenii* strain using the waste from beer fermentation broth. *Carbohydrate Polymers*, 73, 438–445.

Khattak, W. A., Khan, T., Ul-Islam, M., Ullah, M. W., Khan, S., Wahid, F., & Park, J. K. (2015). Production, characterization and biological features of bacterial

cellulose from scum obtained during preparation of sugarcane jaggery (gur). *Journal of Food Sciences and Technology*, 52, 8343–8349.

Kim, J., Cai, Z., Lee, H. S., Choi, G. S., Lee, D. H., & Jo, C. (2011). Preparation and characterization of a bacterial cellulose/chitosan composite for potential biomedical application. *Journal of Polymer Research*, 18, 739–744.

Klemm, D., Schumann, D., Udhardt, U., & Marsch, S. (2001). Bacterial synthesized cellulose artificial blood vessels for microsurgery. *Progress in Polymer Science*, 26, 1561–1603.

Lee, H. S., & Hong, J. (2000). Chemical synthesis and characterization of polypyrrole coated on porous membranes and its electrochemical stability. *Synthetic Metals*, 113, 115–119.

Li, H. X., Kim, S. J., Lee, Y. W., Kee, C. D., & Oh, I. K. (2011). Determination of the stoichiometry and critical oxygen tension in the production culture of bacterial cellulose using saccharified food wastes. *Korean Journal of Chemical Engineering*, 28, 2306–2311.

Marins, J. A., Soares, B. g., Dahmouche, K., Ribeiro, S. J. L., Barud, H., & Denise B. (2011). Structure and properties of conducting bacterial cellulose-polyaniline nanocomposites. *Cellulose*, 18, 285–1294.

Maziarz, E. P., Lorenz, S. A., White, T. P., & Wood, T. D. (2000). Polyaniline: a conductive polymer coating for durable nanospray emitters. *Journal of American Society Mass Spectrometry*, 11, 659–663.

Meftahi, A., Khajavi, R., Rashidi, A., Sattari, M., Yazdanshenas, M. E., & Torabi, M. (2010). The effect of cotton gauze coating with microbial cellulose. *Cellulose*, 17, 199–204.

Nogi, M., & H. Yano. (2008). Transparent nanocomposites based on cellulose produced by bacteria offer potential innovation in the electronics device industry. *Advanced Materials*, 20, 1849-1852.

Qaiser, A. A., Hyland, M. M., & Patterson D. A., (2011). Surface and charge transport characterization of polyaniline-cellulose acetate composite membranes. *Journal of Physical Chemistry B*, 115, 1652–61.

Seo, C., Lee, H. W., Suresh, A., Yang, J. W., Jung, J. K., & Kim, Y.-C. (2014). Improvement of fermentative production of exopolysaccharides from *Aureobasidium pullulans* under various conditions. *Korean Journal of Chemical Engineering*, 31, 1433–1437.

Shah, N., Ha, J. H., & Park, J. K. (2010). Effect of reactor surface on production of bacterial cellulose and water soluble oligosaccharides by *Gluconacetobacter hansenii* PJK. *Biotechnology and Bioprocess Engineering*, 15, 110–118.

Shezad, O., Khan, S., Khan, T., & Park, J. K. (2010). Physicochemical and mechanical characterization of bacterial cellulose produced with an excellent productivity in static conditions using a simple fed-batch cultivation strategy. *Carbohydrate Polymers*, 82, 173–180.

Shi, Z., Gao, X., Ullah, M. W., Li, S., Wang, Q., & Yang, G. (2016). Electroconductive natural polymer-based hydrogels. *Biomaterials*, 111, 40-54.

Shi, Z., Zang, S., & Jiang, F. (2012). *In situ* nano-assembly of bacterial cellulose polyaniline composites. *RSC Advances*, 2, 1040-1046.

Trovatti, E., Oliveira, L., Freire, C. R. (2010). Novel bacterial cellulose-acrylic resin nanocomposites. *Composites Science and Technology*, 70, 1148–1153.

Ul-Islam, M., Khan, S., Ullah, M. W., & Park, J. K. (2015). Bacterial cellulose composites: Synthetic strategies and multiple applications in bio-medical and electro-conductive fields. *Biotechnology Journal*, 10, 1847–1861.

Ul-Islam, M., Khattak, W. A., Kang, M., Kim, S. M., Khan, T., & Park, J. K. (2013). Effect of post-synthetic processing conditions on structural variations and applications of bacterial cellulose. *Cellulose*, 20, 253–263.

Ul-Islam, M., Khattak, W. A., Ullah, M. W., Khan, S., & Park, J. K. (2014). Synthesis of regenerated bacterial cellulose–zinc oxide nanocomposite films for biomedical applications. *Cellulose*, 21, 433–447.

Ul-Islam, M., Shah, N., Ha, J. H., & Park, J. K. (2011). Effect of chitosan penetration on physico-chemical and mechanical properties of bacterial cellulose. *Korean Journal of Chemical Engineering*, 28, 1736–1743.

Ullah, M. W., Ul-Islam, M., Khan, S., Kim, Y., Jang, J. H., & Park, J. K. (2016b). *In situ* synthesis of a bio-cellulose/titanium dioxide nanocomposite by using a cell-free system. *RSC Advances*, 6, 22424–22435.

Ullah, M. W., Ul-Islam, M., Khan, S., Kim, Y., & Park, J. K. (2015). Innovative production of bio-cellulose using a cell-free system derived from a single cell line. *Carbohydrate Polymers*, 132, 286–294.

Ullah, MW., Ul-Islam, M., Khan, S., Kim, Y., & Park, J. K. (2016a). Structural and physico-mechanical characterization of bio-cellulose produced by a cell-free system. *Carbohydrate Polymers*, 136, 908–916.

Ullah, M.W., Khattak, W. A., Ul-Islam, M., Khan, S., & Park, J. K. (2016b). Metabolic engineering of synthetic cell-free systems: Strategies and applications. *Biochemical Engineering Journal*, 105, 391-405.

Wang, H., Zhu, E., Yang, J., Zhou, P., Sun, D., & Tang, W. (2012). Bacterial cellulose nanofiber supported polyaniline nanocomposites with flake-shaped morphology as supercapacitor electrodes. *The Journal of Physical Chemistry C*, 116, 13013–1319.

Yang, N., Chen,X., Ren, T., Zhang, P., & Yang, D. (2015). Carbon nanotube based biosensors. *Sensors and Actuators B Chemical*, 207, 690–715.

Yoon, S. H., Jin, H. J., Kook, M. C., & Pyun, Y. R. (2006). Electrically conductive bacterial cellulose by incorporation of carbon nanotubes, *Biomacromolecules*, 7, 1280–1284.

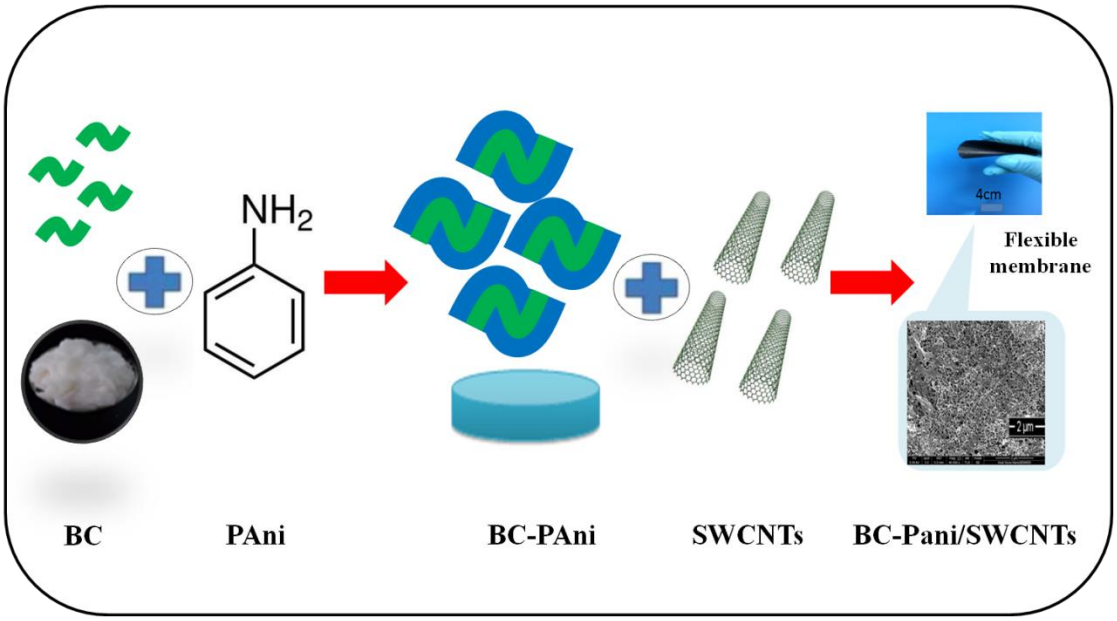

Figure 1. Illustration of BC-PAni/SWCNTs composite synthesis. First a BC-PAni composite was synthesized through oxidative polymerization followed by the *ex situ* addition of different concentrations of SWCNTs.

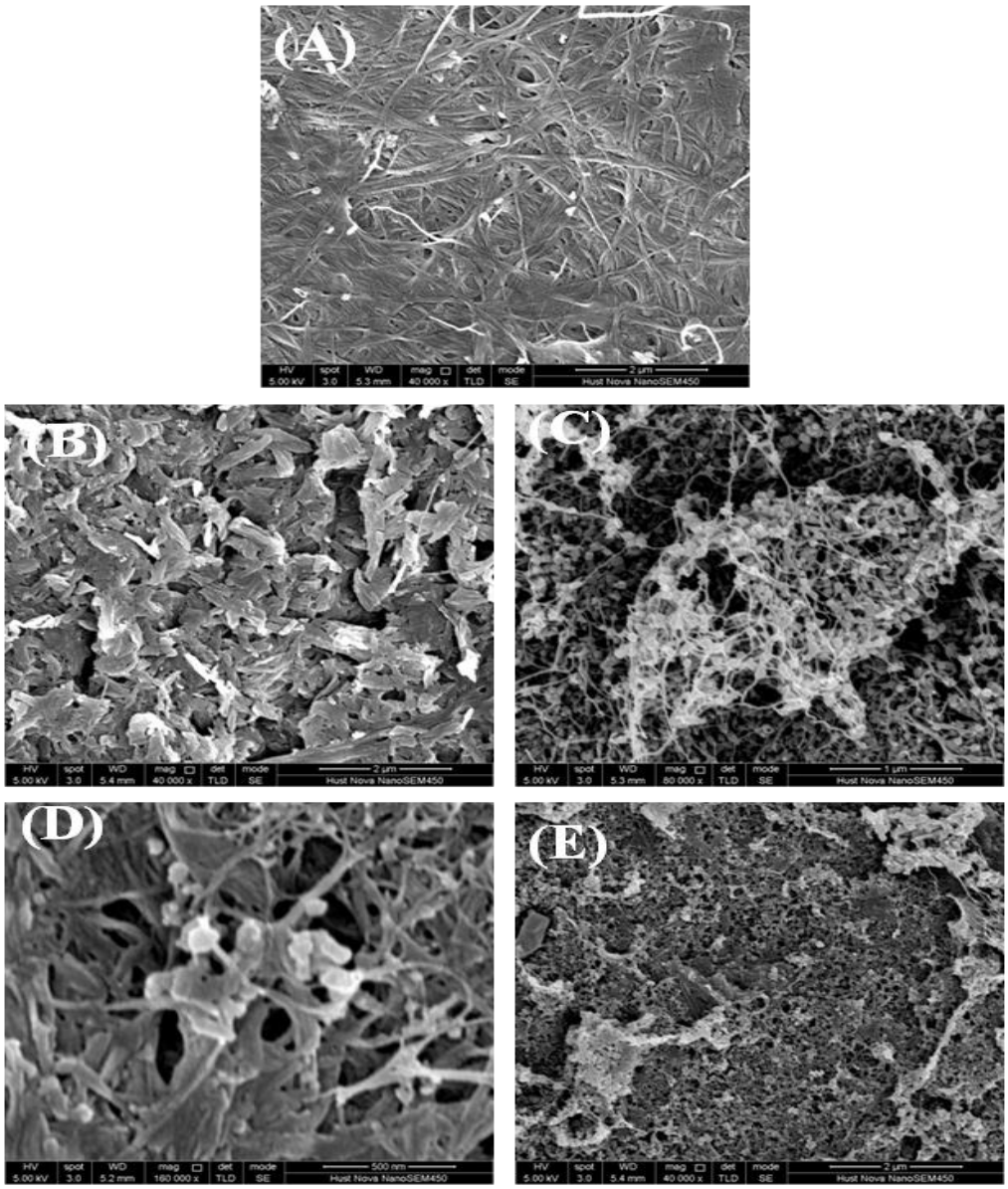

Figure 2. Field-emission scanning electron microscopy images of (A) pure BC pellicles, (B) BC-PAni, (C) purified SWCNTs powder, (D) BC-PAni/SWCNTs-I, and (E) BC-PAni/SWCNTs-II.

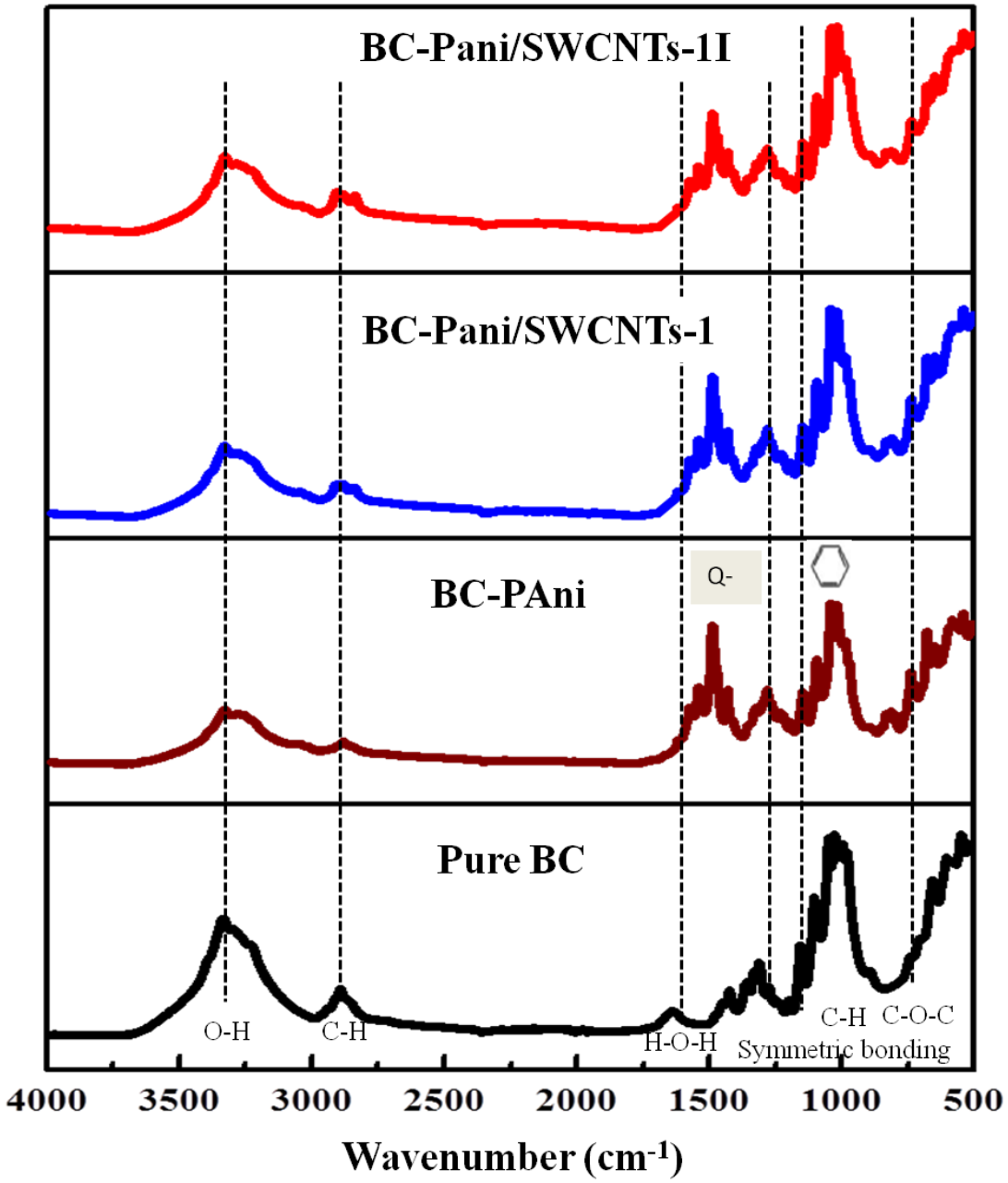

Figure 3. Fourier transform-infrared spectral analysis of pure BC, BC-PAni, BC-PAni/SWCNTs-I and BC-PAni/SWCNTs-II.

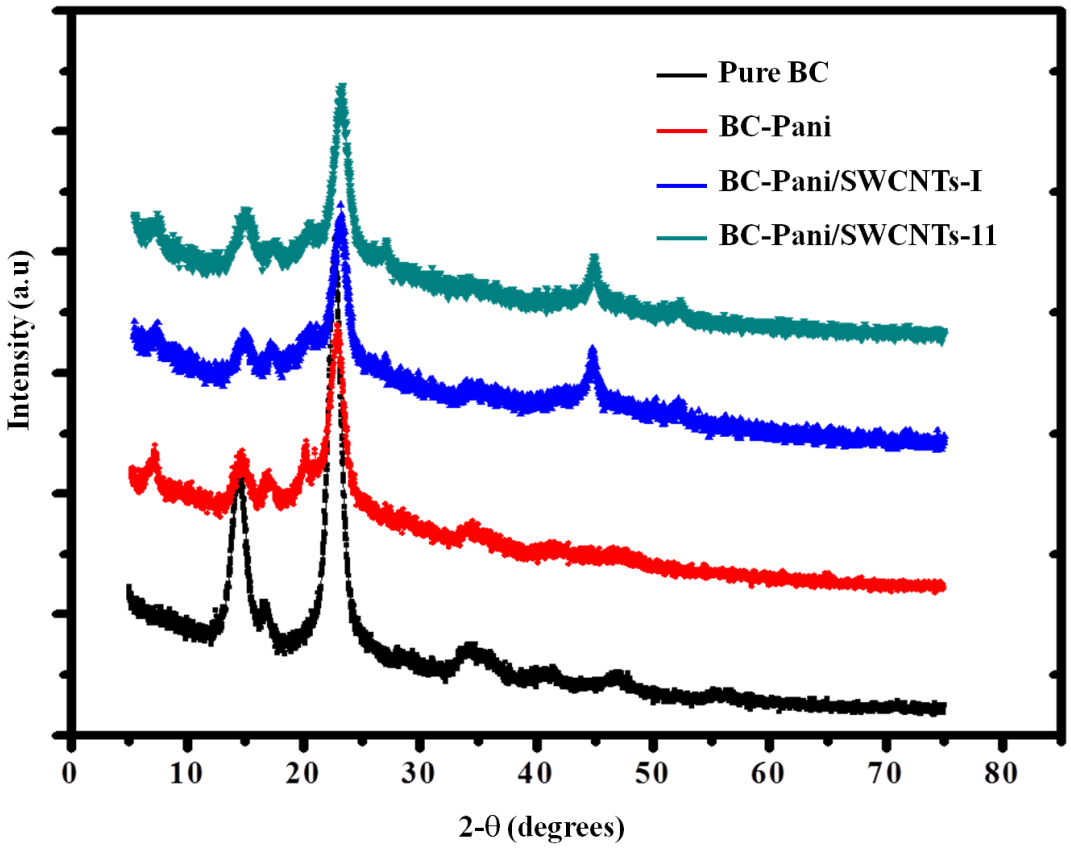

Figure 4. X-ray diffraction patterns of pure BC, BC-PAni, BC-PAni/SWCNTs-I, and BC-PAni/SWCNTs.

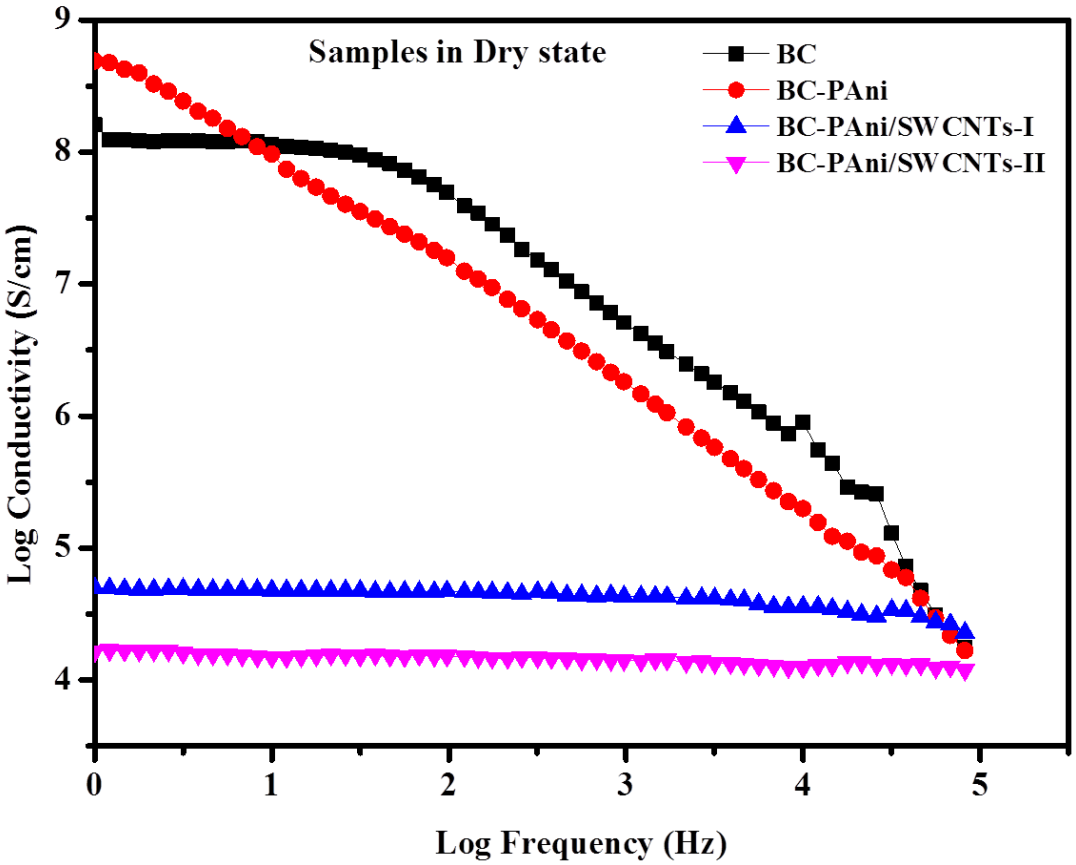

Figure 5A. Electrochemical impedance spectra of the pure BC, BC-PAni, BC-PAni/SWCNTs-I, and BC-PAni/SWCNTs-II membranes. The electrical conductivity of all samples was determined in dry state.

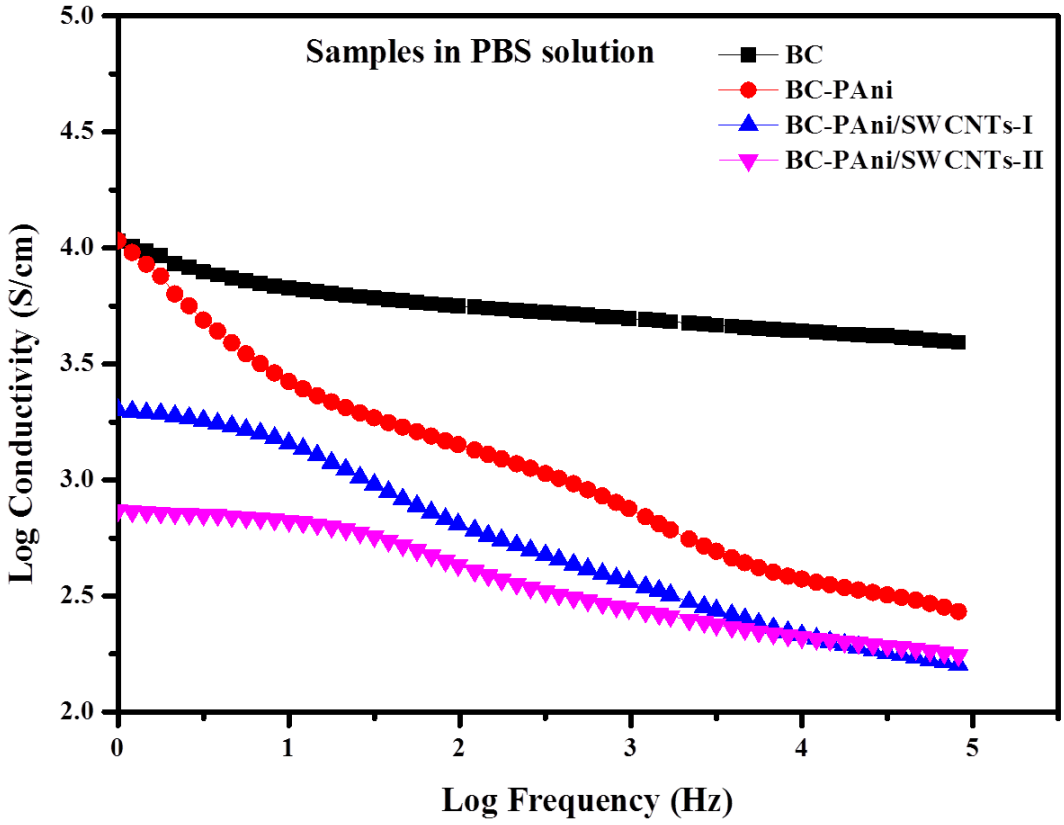

Figure 5B. Electrochemical impedance spectra of the pure BC, BC-PAni, BC-PAni/SWCNTs-I, and BC-PAni/SWCNTs-II membranes. The electrical conductivity of all samples was determined in PBS solution.

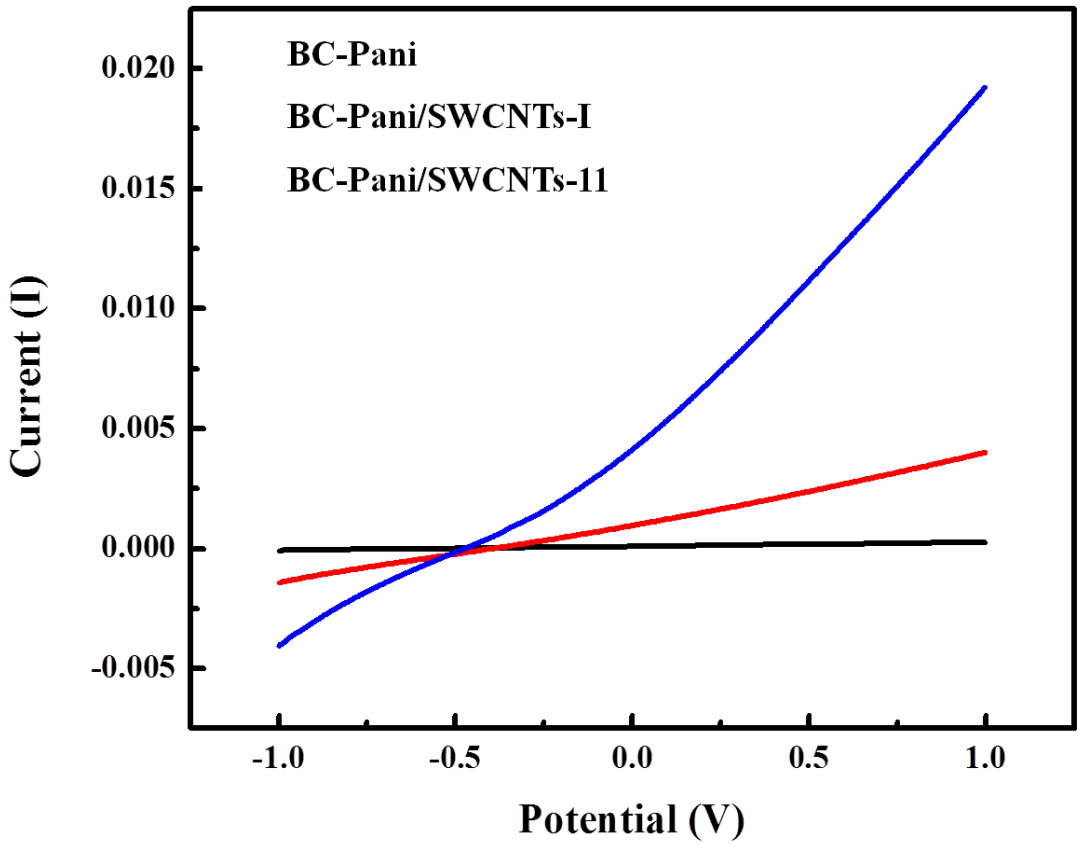

Figure 6. Linear sweep voltammetrograms of BC–PAni with different doping concentrations of SWCNTs. Linear sweep voltammogram of the samples was recorded between two electrodes from –0.1 to 0.1 V for BC-PAni, BC-PAni/SWCNTs-I, and BC-PAni/SWCNTs-II membranes.

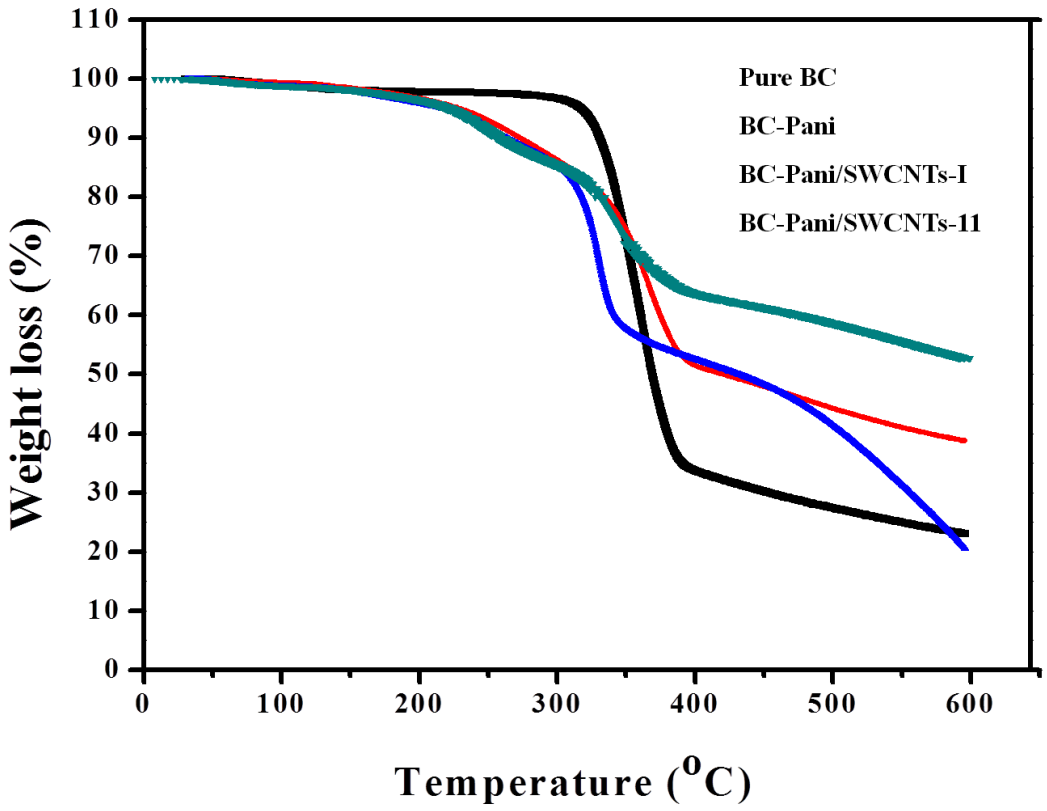

Figure 7. TGA curves of pure BC, BC-PAni, BC-PAni/SWCNTs-I, and BC-PAni/SWCNTs-II membranes.